



HAL
open science

Effects of gas and soot radiation on soot formation in counterflow ethylene diffusion flames

Fs Liu, Hs Guo, Gj Smallwood, Mouna El-Hafi

► **To cite this version:**

Fs Liu, Hs Guo, Gj Smallwood, Mouna El-Hafi. Effects of gas and soot radiation on soot formation in counterflow ethylene diffusion flames. *Journal of Quantitative Spectroscopy and Radiative Transfer*, 2004, 84 (4), pp.501-511. 10.1016/S0022-4073(03)00267-X . hal-01712159

HAL Id: hal-01712159

<https://hal.science/hal-01712159>

Submitted on 14 Nov 2019

HAL is a multi-disciplinary open access archive for the deposit and dissemination of scientific research documents, whether they are published or not. The documents may come from teaching and research institutions in France or abroad, or from public or private research centers.

L'archive ouverte pluridisciplinaire **HAL**, est destinée au dépôt et à la diffusion de documents scientifiques de niveau recherche, publiés ou non, émanant des établissements d'enseignement et de recherche français ou étrangers, des laboratoires publics ou privés.

Effects of gas and soot radiation on soot formation in counterflow ethylene diffusion flames

Fengshan Liu^{a,*}, Hongsheng Guo^a, Gregory J. Smallwood^a, Mouna El Hafib^b

^a*Combustion Technology Group, Institute for Chemical Process & Environmental Technology, National Research Council, Building M9, 1200 Montreal Road, Ottawa, Ontario K1A 0R6, Canada*

^b*Centre Energétique-Environnement, UMR CNRS 2392 Ecole des Mines, d'Albi-Carmaux, 31 all'ees des Sciences, 81000 Albi CT Cedex 09, France*

Abstract

Numerical study of soot formation in counterflow ethylene diffusion flames at atmospheric pressure was conducted using detailed chemistry and complex thermal and transport properties. Soot kinetics was modelled using a semi-empirical two-equation model. Radiation heat transfer was calculated using the discrete-ordinates method coupled with an accurate band model. The calculated soot volume fractions are in reasonably good agreement with the experimental results in the literature. The individual effects of gas and soot radiation on soot formation were also investigated.

Keywords: Gas and soot radiation; Soot formation; Counterflow diffusion flame

1. Introduction

Soot and NO_x formation, gas-phase chemistry, and radiation heat transfer are intimately coupled in flames primarily through the highly nonlinear dependence of these processes on temperature. The importance of the coupling of radiation and soot kinetics in sooting flames has been recognized and demonstrated in several studies [1–3]. Earlier numerical investigations in coflow laminar diffusion flames employed either detailed gas-phase chemistry but the simple optically thin approximation (OTA) for radiation [4–6] or very crude gas-phase chemistry and a more sophisticated treatment for radiation [1,2]. Our recent numerical study [3] was conducted using both detailed gas-phase chemistry and non-grey radiation model in a coflow laminar ethylene diffusion flame with soot modelled using a semi-empirical model. This study found that in a moderately sooting diffusion flame both gas and soot radiation are important in regard to the visible flame height and soot volume fraction.

* Corresponding author. Tel.: +1-613-993-9470; fax: +1-613-957-7869.

E-mail address: fengshan.liu@nrc.cnrc.gc.ca (F. Liu).

Mainly due to the difference in the flame structure, the amount of soot formed in laminar counterflow diffusion flames is much lower than that formed in coflow diffusion flames [7]. Detailed discussions of the effects of the diffusion flame structure on soot formation and oxidation were given in several recent studies [7–9]. Counterflow diffusion flames can be classified into two types: soot formation (SF) flames and soot formation-oxidation (SFO) flames [7,10]. In SF flames the flame appears on the oxidizer side of the stagnation plane and the soot formed in the region between the flame and the stagnation plane is pushed away from the flame toward the stagnation plane by convection and thermophoretic effect. As a result of this specific flame structure, soot oxidation is essentially absent. In SFO flames the flame is formed on the fuel side of the stagnation plane and the soot formed on the fuel side of the flame is transported toward the stagnation plane while undergoing severe oxidation by OH and O₂. Such flames are realized by diluting the fuel stream while enriching the oxidizer stream with oxygen [7–10]. Due to the absence of soot oxidation, soot formation counterflow diffusion flames provide an ideal flame configuration to validate soot surface growth sub-models. The amount of soot formed in SF flames is in general much higher than that in SFO flames and therefore a much stronger coupling between soot process and radiation is expected.

Although soot formation in counterflow diffusion flames has been extensively studied experimentally, relatively few numerical investigations incorporating a soot formation model have been reported [11–14]. In these numerical studies, the effect of radiation heat loss on temperature reduction was either estimated using an empirical correlation to match the experimental temperatures obtained using a thermocouple [11,12] or taken into account by incorporating the radiation heat loss term based on OTA into the energy equation [13,14]. The former treatment of the effect of radiation on temperature must be considered crude for the reason that the temperatures measured by a thermocouple in diffusion flames are in general subject to relatively large errors. While the use of OTA in counterflow diffusion flames at moderate and high stretch rates is adequate, radiation absorption becomes so important at small stretch rates that OTA can cause significant errors for temperature and NO calculations as demonstrated by Wang and Niioka [15] in counterflow CH₄/air diffusion flames. It is therefore expected that radiation absorption should be considered in the prediction of soot formation in counterflow diffusion flames at low stretch. To our best knowledge, detailed numerical studies of the effects of soot and non-grey gas radiation on soot formation in counterflow diffusion flames have not been reported. Perhaps the only relevant numerical study was that conducted by Hall [16] who employed a wide-band model for gas-band radiation with radiation from soot accounted for. Although this study provided some insight into the importance of soot and gas radiation in counterflow diffusion flames, the results can only be regarded as highly qualitative since a rather artificial uniform soot layer was assumed. Moreover, the effect of radiation heat transfer on soot kinetics was not accounted for. There is therefore a need to incorporate an accurate and efficient radiation model into a flame code, such as the CHEMKIN based code used in our previous study [17], to improve the accuracy of temperature calculation, which is essential to soot and NO_x prediction.

Since the first application of the hybrid statistical narrow-band correlated-*k* (SNBCK) method to thermal radiation calculations by Goutière et al. [18], the efficiency of this method has been drastically improved as summarized in a recent study by Liu et al. [19]. In the present study, numerical calculations of soot formation in counterflow ethylene diffusion flames at atmospheric pressure were conducted using a CHEMKIN based code and detailed gas-phase chemistry. The soot model employed was essentially that used in our previous study [3]. Radiation was calculated using the DOM/SNBCK method. The objectives of this study are: (1) to investigate the effects of

radiation and the individual influence of gas and soot radiation on soot formation in counterflow C_2H_4 SF diffusion flames, and (2) to examine the adequacy of the semi-empirical soot model we used previously [3], which was tuned for a coflow C_2H_4 flame, in the modelling of soot formation in counterflow C_2H_4 flames by comparing the numerical results against available experimental data in the literature.

2. Model formulation and numerical method

2.1. Governing equations

Numerical calculations were carried out to model ethylene diffusion flames formed by two coaxial round jets of fuel and oxidizer streams at atmospheric pressure. Although the system is 2D (axisymmetric), the problem can be transformed into a system of ordinary differential equations (1D) valid along the stagnation-point streamline [20]. The ordinary differential equations of mass, momentum, species, and energy along with boundary conditions were given in detail in [20] and will not be repeated here. The radiation source term was added to the energy equation.

2.2. Soot model

The two-equation soot model used in this study is essentially that used in our previous study to model soot formation in a laminar coflow C_2H_4 diffusion flame [3]. This soot model maintains the major features of the model originally developed by Leung et al. [11] with some modifications described in [3]. The two transport equations along the stagnation-point streamline are given as

$$V \frac{dY_s}{dx} = -\frac{d}{dx} (\rho V_T Y_s) + S_m, \quad (1)$$

$$V \frac{dN}{dx} = -\frac{d}{dx} (\rho V_T N) + S_N, \quad (2)$$

where Y_s is the soot mass fraction and N is the soot number density defined as the particle number per unit mass of mixture. Quantity V_T is the thermophoretic velocity of soot in x (stagnation streamline) direction and is given as

$$V_T = -0.5 \frac{\mu}{\rho T} \frac{dT}{dx}. \quad (3)$$

Although more sophisticated soot nucleation mechanisms incorporating PAH as soot inception species were developed [12,13], the numerical results obtained by Smooke et al. [6] in the calculation of a laminar coflow methane diffusion flame showed that the more sophisticated soot model of Hall et al. [13] did not make appreciable difference in the calculated soot volume fraction compared to the result based on the soot model of Fairweather et al. [21], which was essentially the same soot model proposed by Leung et al. [11] with minor modifications. Therefore, there is currently lack of numerical evidence that the more sophisticated soot models [12,13], though theoretically sound, in general perform better than the simpler C_2H_2 based soot model.

The only difference between the soot model used in this study and that used in [3] lies in the surface growth rate. In this study it was given as $k_2 = 700 \exp(-10064/T)$ [$m^{0.5}/s$]. It is noted that

the pre-exponential constant used here (700) was reduced by a factor of 2.5 compared to that used in the calculation of a coflow C_2H_4 diffusion flame (1750) [3]. The reason for the reduction of the pre-exponential constant will be discussed later.

Although soot oxidation is unimportant in the SF counterflow diffusion flames calculated in this study, soot oxidation by molecule O_2 and radicals OH and O was nevertheless included. Details of the soot oxidation sub-model were given in [3].

2.3. Radiation model

The radiation source term in the energy equation was obtained using the discrete-ordinates method (DOM) in 1D parallel-plate geometry. The T_3 quadrature (9 directions in both the positive and negative x direction) was used for the angular discretisation and spatial discretisation of the radiative transfer equation was achieved using the upwind difference scheme.

The SNBCK based unified band model developed by Liu et al. [19] was employed to obtain the absorption coefficients of the gaseous mixture containing CO , CO_2 and H_2O at each band. The spectral absorption coefficient of soot was assumed to be $5.5f_v\nu$ with f_v being the soot volume fraction and ν the wavenumber. The wide bands considered in the calculations were formed by lumping 10 successive uniform narrowbands of 25 cm^{-1} , giving a bandwidth of 250 cm^{-1} for each wide band. The SNB parameters for CO , CO_2 and H_2O were those compiled by Soufiani and Taine [22] based on line-by-line calculations. Calculations were conducted using both 2- and 4-point Gaussian–Legendre quadrature. The total absorption coefficient of combustion products containing CO , CO_2 , H_2O , and soot was calculated as $\kappa_{ij} = \kappa_{ij,g} + 5.5f_v\nu_i$, where subscript i represents i th band, j the j th Gauss quadrature point, and g gas mixture. Wavenumber ν_i takes the value of the i th band centre. The radiation source term was calculated by summing up contributions of all the 36 wide bands (from 150 to 9150 cm^{-1}) considered in the calculations. Further details can be found in [18,19] and the references cited in [19].

2.4. Numerical method

The transport equations for mass flux, stream function, gas-phase species, temperature, and soot mass fraction were solved using a modified Newton method [20]. The computer code used in this study was a revised version of the code employed in our previous study [17] with soot kinetics and the radiation model incorporated. Interaction between gas-phase chemistry and soot kinetics was coupled through the formation/destruction term in the species equations for the relevant species to the soot process. Correction velocities (thermophoretic velocity for soot) were used to ensure that the mass fractions sum to unity. The soot number density equation was solved using a point iteration method. The gas-phase reaction mechanism used was GRI-Mech 3.0 [23]. Calculations were conducted first without radiation. Once the converged adiabatic solutions were obtained, the flame code was restarted with radiation included to save cpu time.

3. Results and discussions

The computational conditions considered in this study were very close to the experimental conditions of the SF flames of Hwang and Chung [10]. In their SF flame experiments, the separation

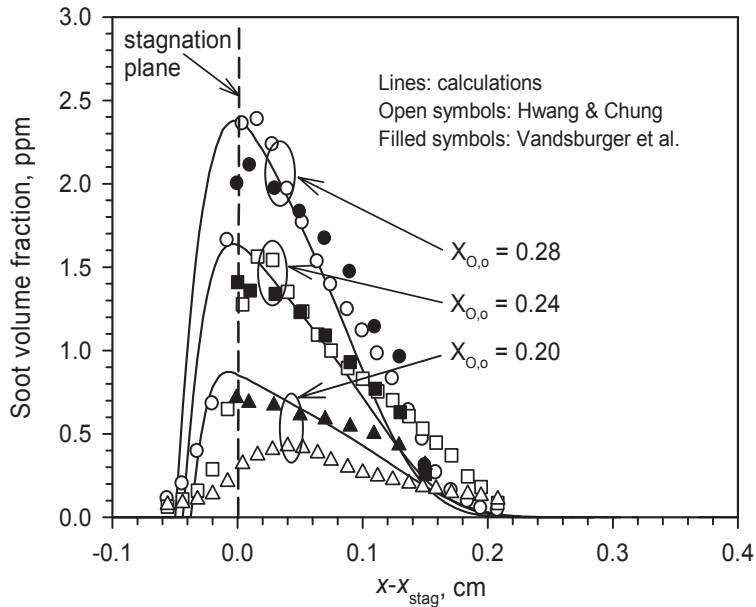


Fig. 1. Comparison between the calculated soot volume fractions and the experimental data.

distance between the fuel (pure C_2H_4) and oxidizer (O_2 balanced by N_2) nozzles was kept at 1.42 cm. Both the fuel and oxidizer were supplied at room temperature. The nozzle exit velocities of both fuel and oxidizer streams were maintained at 19.5 cm/s. In the oxidizer the O_2 mole fraction varied from 20% to 28%. Our numerical experiments indicated that under these conditions the calculated temperature near both the fuel and oxidizer nozzles exhibits small gradient. Consequently it was decided to conduct numerical calculations at a larger nozzle separation distance of 1.7 cm. It was found that an exit velocity of 19.5 cm/s specified at the fuel nozzle (at $x = -0.5$ cm) and a stretch rate of 21 s^{-1} assigned at the oxidizer nozzle (at $x = 1.2$ cm) were adequate to simulate the experiments of Hwang and Chung for all three O_2 mole fractions in the oxidizer, i.e., $X_{O_2,o} = 20\%$, 24% , and 28% .

3.1. Soot model validation

To demonstrate the overall performance of the soot model, the calculated distributions of soot volume fraction are compared with the experimental results of Hwang and Chung [10] for three O_2 concentrations in the oxidizer in Fig. 1. The numerical results were obtained using the DOM/SNBCK radiation model and the 2-point Gauss quadrature. Also plotted in Fig. 1 are the experimental results of Vandsburger et al. [24]. Although the experiments of Vandsburger et al. were conducted under somewhat different conditions compared to those of Hwang and Chung and the present computational conditions, the calculated velocity distributions in these flames (not shown here) indicate that these flames are subject to only slightly lower stretch compared to the experimental velocity distributions of Vandsburger et al. [24]. Therefore, it is valid to include their data in the comparison.

Our preliminary numerical results based on the soot model used in [3] were much higher than the results shown in Fig. 1. A factor of 2.5 reduction in the soot surface growth rate was found necessary to achieve good agreement with the experimental data of Hwang and Chung for $X_{O_2} = 0.28$. It is worth noting that a similar modification (an increase in the surface growth rate by a factor of 2) was also made by Fairweather et al. [25] who applied the very same soot model of Leung et al. [11] to calculate turbulent coflow propane jet diffusion flames. While the exact reason for the reduction of the surface growth rate by a factor of about 2 might be difficult to understand given the semi-empirical nature of the soot model, the following two factors are believed to be partially responsible for this modification. First, the experimental soot volume fractions used in the evaluation of the soot model in the coflow ethylene diffusion flame [3] and considered here in counterflow flames [10] were obtained by two different groups using the laser light extinction technique operated at different wavelengths and different values of the soot absorption constant. It is well known that the soot absorption constants in the visible and near infrared are subject to significant uncertainty [26] and any inconsistency in the soot constant used by the two groups leads to inconsistent soot volume fraction. Secondly, in the calculation of soot volume fraction in laminar coflow diffusion flames, soot oxidation plays an important role in determining the peak soot volume fraction and the visible flame height. To a certain extent, the overprediction of soot surface growth rate can be compensated by using a larger soot oxidation rate, since the net results are the competition between these two processes. This observation highlights the drawback of testing a soot model only in coflow diffusion flames. Numerical evidence exists [27] that the soot oxidation rate by OH suggested by Moss et al. [28], which was also used in [3], could overpredict the actual oxidation rate by a factor of 6. Nevertheless, further experimental and numerical studies are required to ascertain why the surface growth rate has to be reduced by a factor of 2 when the flame configuration is changed from coflow to counterflow.

With the surface growth rate reduced by a factor of 2.5 (tuned for $X_{O_2} = 0.28$) the calculated soot volume fractions are also in reasonably good agreement with the data of Hwang and Chung for $X_{O_2} = 0.24$, but are significantly higher than their data for $X_{O_2} = 0.20$. However, the calculated soot volume fractions are consistently in reasonably good agreement with the experimental data of Vandsburger et al. [24] for all three O_2 concentrations in the oxidizer. It is therefore suggested that the data of Hwang and Chung [10] for $X_{O_2} = 0.2$ should be used with caution. With this observation in mind, the overall agreement between the prediction and the experimental data is regarded as quite good for all three O_2 concentrations. The soot model is capable of predicting correctly the variation of soot volume fraction with oxygen concentration in the oxidizer.

3.2. *Effects of radiation*

The calculated temperature distributions with and without radiation are shown in Fig. 2. As the O_2 concentration increases in the oxidizer not only the peak temperature increases, the location of the peak temperature shifts towards the oxidizer nozzle and the flame becomes thicker. Radiation heat loss has similar effects to decreasing the oxygen concentration in the oxidizer, i.e. to reduce the peak temperature, to shift the location of the peak temperature slightly to the fuel nozzle, and to narrow the flame. The peak temperature reduction by radiation heat transfer is respectively 30, 39, and 50 K for $X_{O_2} = 0.2$, 0.24, and 0.28. It can also be seen that the effect of radiation absorption is insignificant in these flames as the peak temperature based on OTA

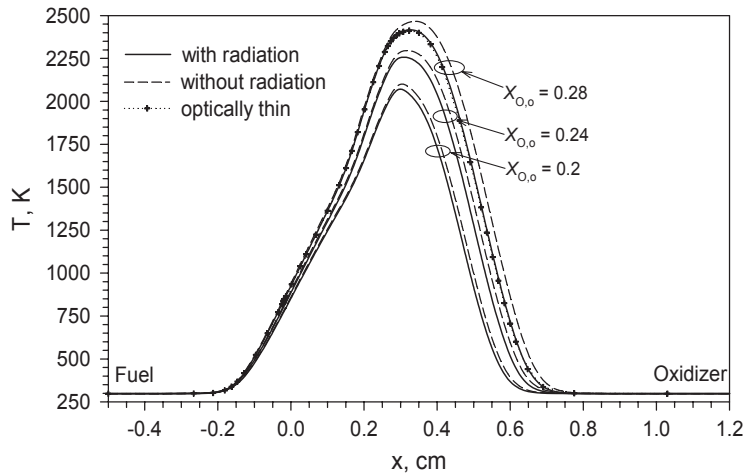


Fig. 2. Effect of radiation on temperature distributions in the three flames investigated.

(without the absorption term) for $X_{O_{2,o}} = 0.28$ is only about 4 K lower than that with the absorption term.

The calculated peak temperatures in these three flames are about 2072, 2257, and 2418 K for $X_{O_{2,o}} = 0.2$, 0.24, and 0.28, respectively. These peak values are about 250 K higher than those measured by Vandsburger et al. [24] using a thermocouple. While the slightly higher stretch rate experienced by the experimental flames in [24] is partially responsible for such a difference in the peak temperatures, they are mainly attributed to the thermocouple errors.

The distributions of soot volume fraction calculated with and without radiation are compared in Fig. 3. Although the absolute reduction of soot volume fractions by radiation increase significantly with increasing oxygen concentration in the oxidizer, it is interesting to note that the relative reduction of the peak soot volume fraction by radiation is about 18% for all three oxygen concentrations considered. Radiation absorption has a negligibly small effect on the calculated SVF, as already seen in the calculated temperature distribution shown in Fig. 2. Even though radiation absorption is not important in the flames calculated in this study at a moderate stretch rate, it becomes important at smaller stretch rates and the radiation model employed here can readily be used to investigate the quantitative effect of radiation absorption. The computed SVF is very sensitive to temperature. Therefore, accurate calculation of radiation heat transfer is important to the prediction of soot.

The effect of radiation on quantities related to soot kinetics are summarized in Fig. 4 for $X_{O_{2,o}} = 0.28$. These results indicate that the reduction of soot volume fraction by radiation is primarily a direct consequence of lowered soot surface growth rate, as the nucleation rate is about two orders of magnitude smaller and the rates of soot oxidation by O_2 and OH are essentially negligible. Both the reduced temperature and the lowered C_2H_2 concentration by radiation heat loss lead to decreased surface growth rates. It is interesting to note that the peak surface growth rate is also reduced by about 18%, in consistent with the relative reduction of the peak soot volume fraction. This is expected in view of the dominant contribution of surface growth process to the soot mass. Although the soot surface growth rate peaks near the middle between the stagnation plane ($x = 0.0325$ cm) and

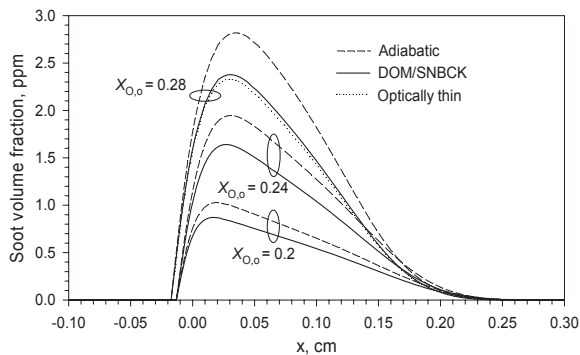


Fig. 3. Effect of radiation on the calculated soot volume fraction distributions.

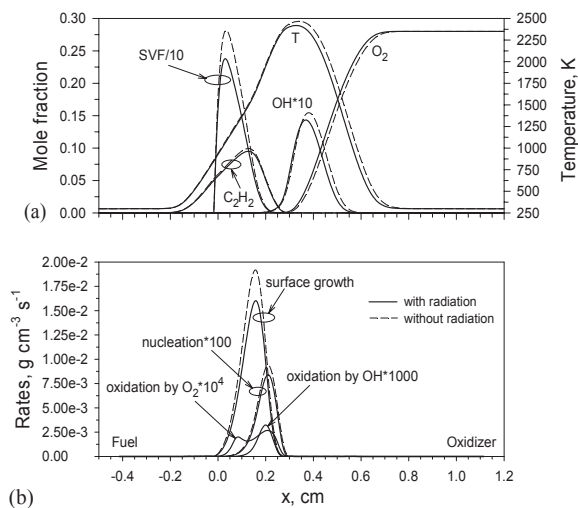


Fig. 4. Effect of radiation on quantities related to soot kinetics in the flame of $X_{O_2,o} = 0.28$.

the location of peak temperature, the soot volume fraction actually peaks almost at the stagnation plane as a result of the combined effect of convection and thermophoretic velocity.

3.3. Relative effect of gas and soot radiation

The relative importance of gas and soot radiation on the calculated soot volume fraction was investigated for the highest oxygen concentration flame. The calculated distributions of the mole fractions of CO, CO₂, and H₂O, the soot volume fraction, and temperature are shown in Fig. 5 based on the DOM/SNBCK radiation model. The concentrations of the two most important radiating gases, CO₂ and H₂O, peak in the same region where the flame temperature exhibits the maximum value. However, the soot volume fraction peaks in a region of significantly lower temperature, only about 1100 K. These observations imply that gas and soot radiation play different roles in affecting the flame structure since they take place in different regions of the flame. Such a specific flame structure also implies that gas radiation is always important regardless the level of soot volume fraction. This flame structure is quite different from that of a coflow ethylene diffusion flame where soot volume fraction peaks in a region of much higher temperatures of about 1600 K [3]. As a result of this difference, soot radiation is less important in these SF counterflow flames compared to their counterparts in coflow configuration on the basis of per soot volume fraction.

The relative importance of gas and soot radiation to the calculated soot volume fraction in the flame of $X_{O_2,o} = 0.28$ is shown in Fig. 6. Although the soot volume fractions in this flame are relatively high, it is interesting to see that gas radiation has a stronger influence in reducing the flame temperature and the soot volume fraction, Fig. 6(a). Actually the peak flame temperature reduction is primarily caused by gas radiation, soot radiation only slightly lowers the peak flame temperature. When both gas and soot radiation are accounted for, the radiation source term has

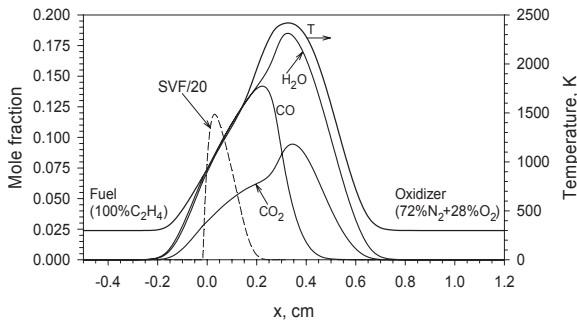


Fig. 5. Distributions of radiating species concentration and temperature for $X_{O_2,0} = 0.28$.

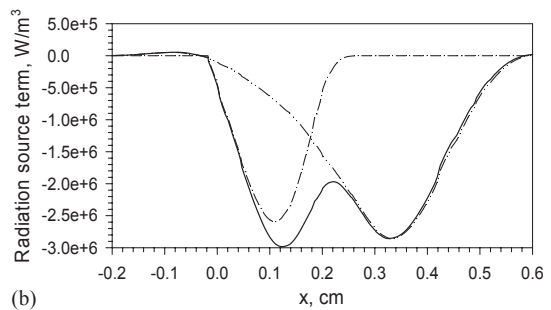
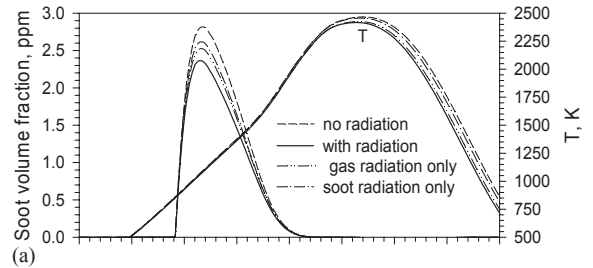


Fig. 6. Individual effect of gas and soot radiation in the flame of $X_{O_2,0} = 0.28$.

two valleys: one is due to gas radiation at the peak temperature region and the other is due to soot radiation at $x = 0.125$ cm, where the temperature is about 1500 K, Fig. 6(b). Results of temperatures shown in Figs. 2 and 6(a) indicate that radiation significantly lowers the temperature on the oxidizer side of flame but otherwise has negligible impact on the temperature on the fuel side of the flame. These results are a consequence of the boundary conditions specified in which the velocity at the fuel nozzle is fixed and the velocity at the oxidizer nozzle is calculated. That is why the location of the peak temperature shifts toward the fuel nozzle when radiation is taken into account.

3.4. Distributions of the radiation source term

Distributions of the radiation source term calculated using the DOM/SNBCK method and the ray-tracing/SNB approach are compared in Fig. 7. It should be pointed out that the SNB results were calculated uncoupled from the flame code by taking the results of the DOM/SNBCK based on the 2-point Gauss quadrature, due to excessive cpu time required by this method. Results of the DOM/SNBCK method, with either 2- or 4-point Gauss quadrature, were obtained from the coupled calculation. Good to excellent agreement is found between the SNBCK method and the SNB model, especially when the 4-point Gauss quadrature was used. Radiation absorption is relatively unimportant even in the flame of $X_{O_2,0} = 0.28$. The double valley structure of the distribution is not very evident in the flame of $X_{O_2,0} = 0.2$, but becomes clear as the oxygen concentration in the oxidizer increases, due to increased soot volume fraction and higher flame temperature.

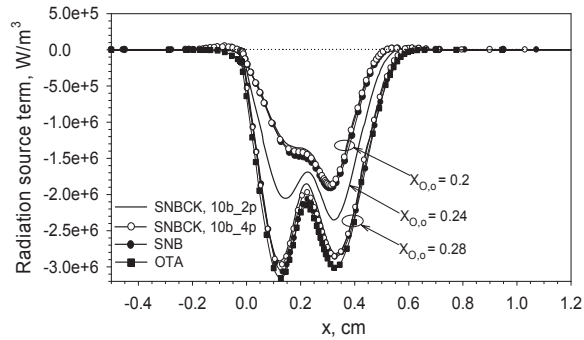


Fig. 7. Radiation source term distributions in the three flames investigated.

4. Conclusions

Numerical study of the effects of gas and soot radiation on soot formation in counterflow ethylene diffusion flames was conducted using detailed gas-phase reaction mechanism, complex transport and thermal properties, a simplified two-equation soot model, and an accurate non-grey radiation model. Numerical results show that the soot model is capable of reproducing the experimental soot volume fractions with reasonably good agreement for different oxygen concentrations in the oxidizer. Gas radiation plays a more important role than soot radiation in affecting flame temperature and soot volume fraction in these soot formation counterflow diffusion flames. Unlike in a coflow diffusion flame where soot volume fraction peaks in a region of relatively high temperature of 1600 K, soot volume fraction peaks in the stagnation plane where the temperature is only about 1000 K in the flames studied. As a result, soot radiation in these counterflow diffusion flames is less important compared to that in coflow flames on the basis of per unit soot volume fraction. The distribution of the radiation source term exhibits a double-valley structure: one is due to gas radiation in the peak flame temperature region and the other is due to soot radiation at a much lower temperature. Further numerical and experimental studies are required to ascertain why a factor of 2 reduction in the soot surface growth rate is needed when the flame configuration is changed from coflow to counterflow.

References

- [1] Sivathanu YR, Gore JP. Coupled radiation and soot kinetics calculations in laminar acetylene/air diffusion flames. *Combust Flame* 1994;97:161–72.
- [2] Sivathanu YR, Gore JP. Effects of gas-band radiation on soot kinetics in laminar methane/air diffusion flames. *Combust Flame* 1997;110:256–63.
- [3] Liu F, Guo H, Smallwood GJ, Gülder ÖL. Effects of gas and soot radiation on soot formation in a coflow laminar ethylene diffusion flame. *JQSRT* 2002;73:409–21.
- [4] Kennedy IM, Yam C, Rapp DC, Santoro RJ. Modeling and measurements of soot and species in a laminar diffusion flame. *Combust Flame* 1996;107:368–82.
- [5] Kaplan CR, Baek SW, Oran ES, Ellzey JL. Dynamics of a strongly radiating unsteady ethylene jet diffusion flame. *Combust Flame* 1994;96:1–21.
- [6] Smooke MD, Mcenally CS, Pfefferle LD, Hall RJ, Colket MB. Computational and experimental study of soot formation in a coflow, laminar diffusion flame. *Combust Flame* 1999;117:117–39.

- [7] Kang KT, Hwang JY, Chung SH, Lee W. Soot zone structure and sooting limit in diffusion flames: comparison of counterflow and co-flow flames. *Combust Flame* 1997;109:266–81.
- [8] Du J, Axelbaum RL. The effect of flame structure on soot-particle inception in diffusion flames. *Combust Flame* 1995;100:367–75.
- [9] Atreya A, Zhang C, Kim HK, Suh J. The effect of changes in the flame structure on the formation and destruction of soot and NO_x in radiating diffusion flames. *Proc Combust Inst* 1996;26:2181–9.
- [10] Hwang JY, Chung SH. Growth of soot particles in counterflow diffusion flames of ethylene. *Combust Flame* 2001;125:752–62.
- [11] Leung KM, Lindstedt RP, Jones WP. A simplified reaction mechanism for soot formation in non-premixed flames. *Combust Flame* 1991;87:289–305.
- [12] Lindstedt PR. Simplified soot nucleation and surface growth steps for non-premixed flames. In: Bockhorn H, editor. *Soot formation in combustion—mechanisms and models*. Springer, Berlin, 1994.
- [13] Hall RJ, Smooke MD, Colket MB. Predictions of soot dynamics in opposed jet diffusion flames. In: Dryer FL, Sawyer RF, editors. *Physical and chemical aspects of combustion*. London: Gordon and Breach; 1997.
- [14] Beltrame A, Porshnev P, Merchan-Merchan W, Saveliev A, Fridman A, Kennedy LA, Petrova O, Zhdanok S, Amouri F, Charon O. Soot and NO formation in methane-oxygen enriched diffusion flames. *Combust Flame* 2001;124:295–310.
- [15] Wang J, Niioka T. The effect of radiation reabsorption on NO formation in CH_4/air counterflow diffusion flames. *Combust Theory Modelling* 2001;5:385–98.
- [16] Hall RJ. Radiative dissipation in planar gas-soot mixtures. *JQSRT* 1994;51:635–44.
- [17] Liu F, Guo H, Smallwood GJ, Gülder ÖL. The chemical effects of carbon dioxide as an additive in an ethylene diffusion flame: implications for soot and NO_x formation. *Combust Flame* 2001;125:778–87.
- [18] Goutière V, Liu F, Charette A. An assessment of real-gas modelling in 2D enclosures. *JQSRT* 2000;64:299–326.
- [19] Liu F, Smallwood GJ, Gülder ÖL. An accurate efficient and flexible SNBCK-based unified band model for calculations of spectrally resolved and integrated quantities in participating media containing real-gases. *Proceedings of the 12th International Heat Transfer Conference, 2002*. Genalpe, France, Aug 18–23. p. 663–8.
- [20] Smooke MD, Puri IK, Seshadri K. A comparison between numerical calculations and experimental measurements of the structure of a counterflow diffusion flame burning diluted methane in diluted air. *Proc Combust Inst* 1986;21:1783–92.
- [21] Fairweather M, Jones WP, Lindstedt RP. Predictions of radiative transfer from a turbulent reacting jet in a cross-wind. *Combust Flame* 1992;89:45–63.
- [22] Soufiani A, Taine J. High temperature gas radiative property parameters of statistical narrow-band model for H_2O , CO_2 and CO , and correlated- K model for H_2O and CO_2 . *Int J Heat Mass Transfer* 1997;40:987–91.
- [23] Smith GP, Golden DM, Frenklach M, Moriarty NW, Eiteneer B, Goldenberg M, Bowman CT, Hanson RK, Song S, Gardiner Jr WC, Lissianski VV, Qin Z. http://www.me.berkeley.edu/gri_mech/.
- [24] Vandsburger U, Kennedy I, Glassman I. Sooting counterflow diffusion flames with varying oxygen index. *Combust Sci Technol* 1984;39:263–85.
- [25] Fairweather M, Jones WP, Ledin HS, Lindstedt RP. Predictions of soot formation in turbulent non-premixed propane flames. *Proc Combust Inst* 1992;24:1067–74.
- [26] Krishnan SS, Lin K-C, Faeth GM. Extinction and scattering properties of soot emitted from buoyant turbulent diffusion flames. *J Heat Transfer* 2001;123:331–9.
- [27] Ezekoye OA, Zhang Z. Soot oxidation and agglomeration modeling in a microgravity diffusion flame. *Combust Flame* 1997;110:127–39.
- [28] Moss JB, Stewart CD, Young KJ. Modeling soot formation and burnout in a high temperature laminar diffusion flame burning under oxygen-enriched conditions. *Combust Flame* 1995;101:491–500.